Nuclear reaction rate uncertainties and astrophysical modeling: Carbon yields from low-mass giants

Falk Herwig,[1,*] Sam M. Austin,[2,†] and John C. Lattanzio[3,‡]

[1]*Los Alamos National Laboratory, Theoretical Astrophysics Group in T-Division, MS B227, Los Alamos, New Mexico 87545, USA*

[2]*National Superconducting Cyclotron Laboratory and Joint Institute for Nuclear Astrophysics, Michigan State University, East Lansing, Michigan 48824, USA*

[3]*School of Mathematical Sciences, Monash University, Wellington Road, Clayton, Vic 3800, Australia*

(Received 17 May 2005; published 13 February 2006)

Calculations that demonstrate the influence of three key nuclear reaction rates on the evolution of asymptotic giant branch stars have been carried out. We study the case of a star with an initial mass of 2 $M_\odot$ and a metallicity of $Z = 0.01$, somewhat less than the solar metallicity. The dredge-up of nuclear processed material from the interior of the star and the yield predictions for carbon are sensitive to the rate of the $^{14}N(p,\gamma)^{15}O$ and triple-α reactions. These reactions dominate the H- and He-burning shells of stars in this late evolutionary phase. Published uncertainty estimates for each of these two rates propagated through stellar evolution calculations cause uncertainties in carbon enrichment and yield predictions of about a factor of 2. The other important He-burning reaction, $^{12}C(\alpha,\gamma)^{16}O$, although associated with the largest uncertainty in our study, does not have a significant influence on the abundance evolution compared with other modeling uncertainties. This finding remains valid when the entire evolution from the main sequence to the tip of the asymptotic giant branch is considered. We discuss the experimental sources of the rate uncertainties addressed here and give some outlooks for future work.

DOI: 10.1103/PhysRevC.73.025802 PACS number(s): 26.20.+f, 97.10.Cv, 97.60.−s

I. INTRODUCTION

Modern computer codes for stellar evolution calculations solve routinely a nuclear reaction network sufficiently large to account for all relevant nuclear transmutations. Reliable nuclear reaction rates are a crucial ingredient for accurate modeling of the evolution of stars, especially for investigations of the chemical evolution of the stars and of the amount of processed material that is returned to the interstellar medium. Such stellar model results are used for integrated models of the galactic chemical evolution and for comparison with individual stellar abundance observations.

In spite of the obvious necessity to check the sensitivity of stellar chemical evolution predictions to uncertainties in the underlying reaction rates, little work in this direction has been done recently [1]. This is, in particular, true for the evolution of low- and intermediate-mass stars ($0.8 < M_\star/M_\odot < 8$) that host important nuclear production sites and contribute significantly to galactic chemical evolution. Two main issues make investigations of the propagation of nuclear reaction-rate uncertainties difficult. One is the computationally expensive and numerically difficult nature of the advanced evolutionary phases of low- and intermediate-mass stars. The second is that such studies are useful only if consistent estimates of the individual rate uncertainties are available.

We have started a program to address this problem. In Ref. [2] we investigated the impact of CNO cycle (p,γ) reaction-rate uncertainties on the predicted stellar oxygen isotopic ratios. These predictions are important for the astrophysical interpretation of presolar meteoritic corundum grains [3,4]. Reference [2] used a Monte Carlo approach integrated into nuclear network postprocessing calculations.

In this second study we focus on the evolution of asymptotic giant branch (AGB) stars and their sensitivity to the rates of three key nuclear reactions: $^{14}N(p,\gamma)^{15}O$, triple-α, and $^{12}C(\alpha,\gamma)^{16}O$. We extend our preliminary results of this project [5] and provide a more in-depth presentation. The sections describe the following topics: Sec. II, astrophysical background; Sec. III, nuclear physics input, its uncertainties, and possible revisions; Sec. IV, the physical model and methods of the astrophysics simulation, as well as the main elements of AGB evolution that are important here; Sec. V, our results as well as additional calculations with a second, independent code that verify the findings; Sec. VI, new results for the triple-α rate; and Sec. VII, results and discussion.

II. ASTROPHYSICAL CONTEXT

After the initial H- and He-core-burning phases, low- and intermediate-mass stars evolve into double-shell-burning giant stars [6,7]. These AGB stars have a unique mechanical structure, as explained in more detail in Ref. [8]. The electron-degenerate core with mass $M_c \approx 0.6\ M_\odot$ consists of carbon and oxygen (the ashes from previous evolutionary phases) and is about the size of the earth, while the envelope has on average roughly the density of water and extends to several hundred times the radius of the sun. This envelope is unstable against convection and is thus well mixed.

Recurrent He-shell flashes, with periods of $5–10 \times 10^4$ yr, are a characteristic of these configurations. A combination of partial degeneracy, the small geometric scale of the He-burning shell, and the strong temperature dependence of the triple-α reaction rate leads to a thermonuclear runaway that locally generates power of roughly 10^{34}W ($10^8 L_\odot$). Neither heat conduction nor photon radiation is sufficient to carry away

*Electronic address: fherwig@lanl.gov
†Electronic address: austin@nscl.msu.edu
‡Electronic address: John.Lattanzio@sci.monash.edu.au

the energy, and the layer between the He- and the H-shell becomes convectively unstable.

Part of the energy released in the He-flash will do expansion work, cooling the layers above the He-shell. The stellar opacities in this region at the base of the convective envelope then increase, which forces the envelope deep into the core (in terms of the Lagrangian mass coordinate, the enclosed mass). This penetration of the envelope convection zone into the processed core material below the the H-burning shell is the third dredge-up.[1] The details of these events are well documented in the astrophysical literature [9–14].

The dredge-up event is responsible for the transfer of nuclear processed material from the high-temperature stellar interior to the low-temperature stellar surface, where it can be observed spectroscopically. This material is also blown into the interstellar medium by stellar winds. For these reasons, the strength of the dredge-up is of great importance to the observed chemical enrichment of low-mass giants and their role in galactic chemical evolution.

The amount of dredge-up obtained in stellar models of the AGB stars continues to be a matter of debate. It is well established that the dredged-up amount depends on the core mass, the stellar metallicity and opacity, the model of convection, and the treatment of convective boundaries, as well as on the numerical implementation of several details in the codes [15–17]. Earlier studies have already indicated that stronger He-shell flashes are followed by deeper dredge-up [18] and that a decreased energy generation in the H-shell leads to stronger He-shell flashes [19]. However, there are no investigations of the sensitivity of dredge-up and the envelope abundance evolution to nuclear reaction-rate uncertainties.

We focus on the three reactions that dominate H-burning and He-burning. It is well known that the ^{14}N$(p,\gamma)^{15}$O reaction has the smallest rate in the CN cycle; it controls the circulation rate of the CN catalytic material in the H-burning shell. The ^{12}C$(\alpha,\gamma)^{16}$O reaction is weakly active during the interpulse phase between the He-shell flashes. The most important reaction for the He-shell flash is the triple-α reaction.

In double-shell burning around degenerate cores, several competing time scales are involved. The period of the He-shell flashes depends mainly on the rate of He accretion from the H-burning shell. The strength of the He-shell flash depends on the geometrical size and on the partial degeneracy of the He-shell. A more degenerate and thinner shell results from a longer flash period, which in turn can be caused by the smaller energy generation rate that is due to a smaller CNO cycle rate. In such a case it takes longer to accrete the required amount of He from the H-burning shell to ignite the flash. Thus one can qualitatively understand that the H-shell-burning rate influences the He-shell-flash strength and thereby the subsequent dredge-up.

The possible influence of the triple-α reaction on the He-shell-flash strength is perhaps more obvious. A larger rate is likely to cause a larger peak-flash He-burning luminosity and subsequently a deeper dredge-up. Our qualitative expectation is then that a reduced ^{14}N$(p,\gamma)^{15}$O rate and an increased triple-α rate will each increase the amount of carbon produced in the process. The effect of the ^{12}C$(\alpha,\gamma)^{16}$O rate is less obvious. To obtain quantitative estimates on these processes we conducted a detailed numerical study.

III. NUCLEAR PHYSICS INPUT

The NACRE Collaboration [20] recommended reaction rates for the reactions we consider here. In this section we examine whether, six years after their publication, the NACRE estimates still describe the available data with sufficient accuracy for our purposes. Table I lists the temperatures of interest: $T_8 = 0.5\,(T = 5 \times 10^7$ K) to $T_8 = 0.8$ for the ^{14}N$(p,\gamma)^{15}$O reaction and $T_8 = 1$–3 for the triple-α and the ^{12}C$(\alpha,\gamma)^{16}$O reactions.

A. ^{14}N$(p,\gamma)^{15}$O

The ^{14}N$(p,\gamma)^{15}$O reaction has a complex structure with transitions, both resonant and nonresonant, to several final

[1] It follows two dredge-up periods during previous evolutionary phases, which are, however, less important for the overall chemical enrichment of low- and intermediate-mass stars.

TABLE I. Relevant temperature range, NACRE nuclear reaction rates and their uncertainties [20], and adopted factors to fitting formula rates for our calculations.

Reaction	T_8	$\langle\sigma v\rangle_{\rm low}$	$\langle\sigma v\rangle$[a]	$\langle\sigma v\rangle_{\rm high}$	exp[b]	$f_{\rm fit}^{c}$	$f_{\rm up}^{\rm d}$	$f_{\rm low}^{\rm e}$
^{14}N(p,γ)	0.5	2.67	3.68	4.69	−10	0.9701	1.3137	0.7479
	0.8	0.76	1.04	1.32	−7	0.9488	1.3377	0.7702
Adopted for our calculations							1.33	0.75
3α	1.0	2.05	2.38	2.70	−24	1.0424	1.0883	0.8263
	3.0	3.95	4.57	5.18	−13	1.0068	1.1258	0.8585
Adopted for our calculations							1.13	0.82
^{12}C(α,γ)	1.0	1.06	1.81	2.55	−20	0.9762	1.4431	0.5999
	3.0	2.88	4.75	6.62	−12	0.9905	1.4070	0.6121
Adopted for our calculations							1.44	0.60

[a] Recommended reaction rate.

[b] Power of 10 multiplying reaction rates in columns 3, 4, and 5.

[c] Ratio between tabulated value and fit formula.

[d] $\langle\sigma v\rangle_{\rm high}/(\langle\sigma v\rangle f_{\rm fit})$.

[e] $\langle\sigma v\rangle_{\rm low}/(\langle\sigma v\rangle f_{\rm fit})$.

states contributing to the rate. In addition, contributions from the tails of subthreshold states must be considered. In Ref. [21] data were obtained over a wide energy range from 0.2 to 3.6 MeV; the R-matrix fit of Ref. [21] to these data yielded a large S factor for the transitions to the ground state. Their total S factor, $S(0) = 3.2 \pm 0.54$ keV b, was the principal basis for the NACRE reaction rate, 3.2 ± 0.8 keV b [20]. However, the fit to the ground-state cross section required an unusually large value for the γ width of a subthreshold $3/2^+$ state at $E_x = 6.793$ MeV in ^{15}O, about seven times that of the isospin-analog transition in ^{15}N. Such large differences are seldom, if ever, seen, at least for light nuclei [22,23]. Motivated by this fact, direct measurements of the 6.793 state's lifetime were made [24,25] and yielded much smaller γ widths. A reanalysis [26] of the Schroeder data resulted in a much smaller ground-state transition and $S(0) = 1.77 \pm 0.2$ keV b. Later, determinations of asymptotic normalization coefficients (ANCs) for the relevant transitions made by use of nuclear transfer reactions, combined with some of the Schroeder results [27], led to $S(0) = 1.7 \pm 0.41$ keV b.

Recently, additional ^{14}N$(p, \gamma)^{15}$O data and corrected data from Ref. [21] were analyzed to yield $S(0) = 1.70 \pm 0.22$ keV b [28]. An independent measurement at Triangle Universities Nuclear Laboratory (TUNL) [29] yielded $S(0) = 1.68 \pm 0.18$ keV b. Measurements of the analyzing power at 270 keV [30] indicate that $M1$ contributions to the cross section should be considered; to our knowledge these contributions have not been included in detailed fits to the data. There are also preliminary data down to 70 keV [31] for the main transition, that to the 6.79-MeV state.

All the recent investigations show that the ground-state transition is small and that the resulting total S factor is smaller by about a factor of 2 than the NACRE result. In the near future, the reliability of the rate is likely to improve as more complete analyses that include all the recent data are carried out. However, for now we have chosen to use an unweighted average of the four recent results and a conservative error reflecting the relatively long extrapolations to the astrophysical range, the neglect of the $M1$ amplitudes, and the imperfect fits to the data. We obtain $S(0) = 1.70 \pm 0.25$ keV b. For easy employment in the stellar evolution code, this value can be approximated as a fraction $f = 0.64 \pm 0.1$ of NACRE's analytical fit [20] to the reaction rate in the relevant temperature range.

B. Triple-α

The first step of the triple-α process is the fusion of two α particles to form an equilibrium concentration of ^{8}Be. The subsequent capture of an α particle produces an equilibrium concentration of ^{12}C in its 7.65 MeV 0^+ state. Occasionally ^{12}C is formed by a leak, by means of a γ cascade or pair emission, to the ground state of ^{12}C. For the temperatures involved in the present calculations, both of these steps are resonant and the reaction rate is given by

$$r_{3\alpha} \propto \Gamma_{\rm rad} \exp(-Q/kT). \quad (1)$$

The value of Q for the 7.65-MeV state is known to within ± 0.2 keV [32] and contributes an uncertainty in the rate of only $\pm 1.2\%$ for $T_8 = 2$. Essentially all the uncertainty in the rate is due to the uncertainty in $\Gamma_{\rm rad}$, the radiative width of the 7.65-MeV state; $\Gamma_{\rm rad}$ is known with a precision of $\pm 12\%$. It is essentially these established values of $\Gamma_{\rm rad}$ and Q that are incorporated into the NACRE rates for the temperatures considered here, and hence, for our purpose, the NACRE rates are adequate. We shall see, however, that they are not sufficiently accurate.

Following the completion of the calculations described herein, Fynbo *et al.* [33,34] determined the level structure of ^{12}C and concluded from their results that the 7.65-MeV state alone adequately describes the reaction rate for temperatures $T = 0.1$–100×10^8 K. They also concluded that, at $T = 2 \times 10^8$ K, the midpoint of the temperature range covered here, the triple-α rate is smaller than the NACRE results by about 10%. This is comparable with the quoted error we used, and one should keep this in mind when examining the details of the present results. In fact, our calculations can be used to determine the effect of the 10% change on C yields.

C. ^{12}C$(\alpha, \gamma)^{16}$O

This reaction has been the subject of many experiments and analyses over a period of 40 years, but it is still not accurately known. It is not possible here to review this subject in detail, it is simply too complex. One can find a comparison of the various rates in Fig. 1 of Ref. [35], and the references cited there can be consulted for more detail. An extensive discussion of this rate can be found in Ref. [36] and the results of extensive recent measurements in Ref. [37]. The NACRE rate is probably somewhat too large in the region of present interest, but the quoted uncertainties are sufficiently large to represent the probable range of acceptable values. This is a minor issue for the present calculations since, as we shall see, carbon production in low- and intermediate-mass AGB stars is very weakly dependent on the ^{12}C$(\alpha, \gamma)^{16}$O rate.

D. Comments

We conclude that the NACRE recommendations describe current triple-α and ^{12}C$(\alpha, \gamma)^{16}$O data sufficiently well, at least for the temperature range relevant here. Recent data, however, make it clear that the NACRE estimate for the ^{14}N$(p, \gamma)^{15}$O rate is high by roughly a factor of 2.

IV. METHODS AND PHYSICS INPUT

The one-dimensional stellar evolution codes we employed solve the well-established full set of nonlinear partial differential equations to account for hydrostatic equilibrium, mass continuity, and energy transport and generation [14,16,38]. Most of the calculations have been done with the code EVOL [39]. It includes updated input physics.[2] A small amount of

[2]The opacities, for example, are from Ref. [40] supplemented with low-temperature opacities from Ref. [41].

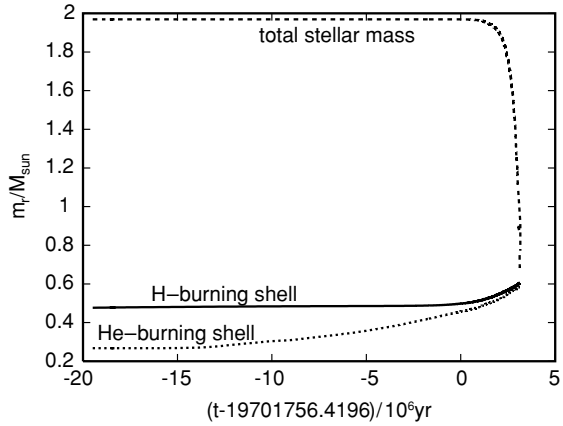

FIG. 1. Evolutions of the Lagrange coordinates of the stellar surface and of the H- and He-burning shells with increasing time. As the star evolves, mass loss increases with time and the total mass decreases. The lines start at the end of He-core burning. Time has been set to zero at the maximum He-burning luminosity of the first He-shell flash.

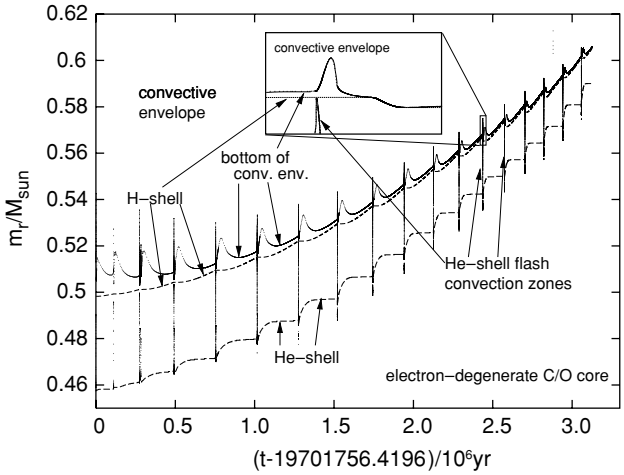

FIG. 2. Similar to Fig. 1, but only for the AGB phase with He-shell flashes. The inset shows the detail of an individual dredge-up event. The inset mass range shown is from 0.56 to 0.58 $M_\odot$ and the time range are from 2.4360×10^6 to 2.4375×10^6 yr. More details of AGB evolution are given in a review article [8].

envelope overshooting, but no overshooting at other AGB convection zones, is introduced following [42].[3]

To generate the initial model for our comparative study we compute the evolution of a star with a mass of $2\,M_\odot$ and a metallicity of $Z = 0.01$ from the pre-main sequence through the H- and He-core-burning phase. After the He-core-burning phase the star gradually climbs up the AGB in the $\log T_{\rm eff} - \log L$ (Hertzsprung-Russell) diagram. We choose as a starting model for all subsequent calculations a model at the very end of the He-core-burning phase and well before the onset of the first He-shell flashes.

The evolutions of the H- and the He-burning shells and of the stellar surface in the Lagrangian mass coordinate for the benchmark sequence ET2 are shown in Fig. 1. From the end of the He-core-burning phase the star spends about 20 million yr on the so-called early-AGB phase. During this phase the H-burning shell is largely inactive and most nuclear energy is produced in the He-burning shell.

He-shell flashes occur only during a rather short period of the post-He-core-burning phase. The underlying reason for their occurrence is the different burning rate of the two shells, which eventually prohibits quiescent double-shell burning. A close-up of the actual He-shell-flash phase of the AGB is shown in Fig. 2. Seventeen thermal pulses can be identified by the vertical lines that connect the H-shell and the He-shell at almost equidistant intervals. These vertical lines are the brief He-shell flash convection zones which last for only 200–300 yr. During the flash the convectively unstable layers are confined to the region below the H-shell and above the He-shell. The inset shows a small spike at the bottom, which is the rapidly growing upper boundary of the He-shell-flash convection zone. It stops just short of the mass coordinate of the H-free core where the H-shell is located and quickly retreats afterward. The H- and He-burning shells remain well separated even during the He-shell-flash episodes, and no H from the envelope can enter the He-burning shell. The inset also shows how the bottom of the convective envelope (CE) later descends into mass layers previously occupied by the He-shell-flash convection zone and with consequent "dredging" of processed material into the envelope. It is this tiny detail in the convective evolution of the stellar interior that is responsible for the enrichment of the envelope and eventually, through mass loss, of the interstellar medium. The dredge-up events after the thermal pulses cause a gradual increase of carbon and, to a much lesser extent, oxygen (Fig. 3). The surface abundance for ^{16}O is nearly constant with time for near-solar metallicity. This results in an increase of the C/O ratio and eventually to the formation of C stars. More detailed figures of the evolution of He-shell flashes can be found, for example, in Fig. 1 and 10 in Ref. [16].

For any comparative study of the propagation of nuclear reaction-rate uncertainties in a stellar evolution code, a somewhat consistent set of quantitative estimates on the uncertainties is required. In the absence of such estimates, one is left with the rather crude approach of applying common factors to all rates in question. However, such an approach misses out on critical aspects of the error propagation in a real stellar evolution environment. As we will show, for example, the reaction in our sample with the largest relative error has the smallest impact on the observable prediction (see also Ref. [2]).

In this study we rely initially on the NACRE compilation [20] that contains recommended values and estimates for lower and upper bounds as functions of temperature. We then consider the impact of the revised recommendation for the ^{14}N$(p,\gamma)^{15}$O reaction. Note that the recommended factors apply in only the given temperature range. In Table I and Fig. 4 we show the relevant information from the NACRE compilation for the two temperature ranges appropriate for

[3]The efficiency for convective envelope overshooting is $f_{\rm ce} = 0.016$; see Ref. [16] for a description of the overshooting scheme used. Mass loss is included by adoption of the formalism of Ref. [14] with a scaling factor $\eta_B = 0.1$. For more details and definitions see Ref. [39].

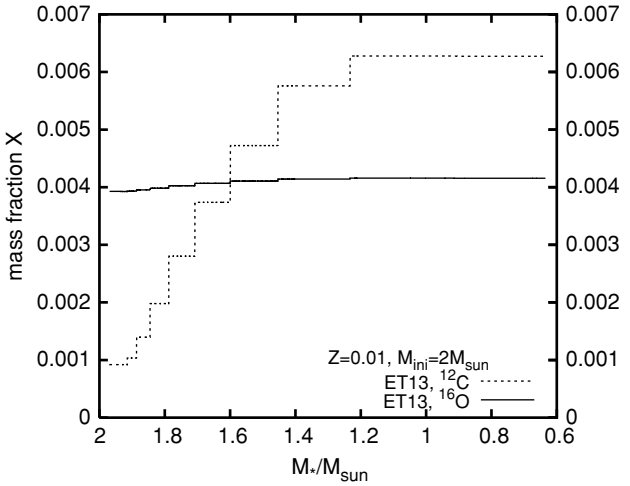

FIG. 3. Evolution of ^{12}C and ^{16}O (in mass fraction) in the envelope (i.e., at the surface) as a function of total stellar mass (sequence ET13). Since the total stellar mass decreases with time, the figure shows the time evolution of the envelope ^{12}C abundance. The intershell material that is dredged up to the envelope contains more C than O, which eventually leads to C star formation (C/O > 1). Integration of the surface abundance over the mass lost gives the ^{12}C yields.

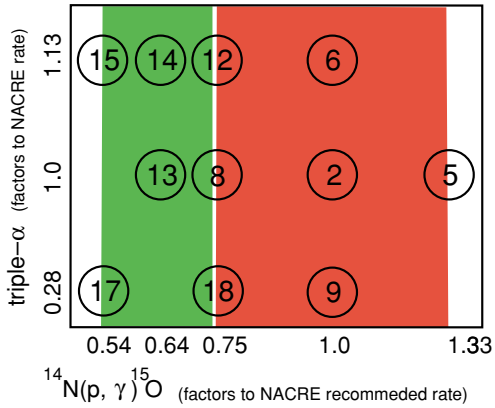

FIG. 4. (Color online) Rate selection for stellar evolution He-shell-flash calculations. The numbers correspond to the sequence numbers in this paper. The red (dark) area corresponds to the NACRE range for the ^{14}N(p,γ) rate, and the green (light) area covers the revised range for this rate for the temperature range considered in this work (see Table I).

He- and H-burning, respectively. In addition to the tabulated reaction rates, fitting formulas for the recommended values are provided. In the calculations we use these formulas instead of tables to evaluate the reaction rates at the required temperatures. We checked the accuracy of the formulas and found that, for the T range of interest here (as indicated in Table I, column 2), the fitting error is rather small, as shown in Column 7 of Table I, which shows $f_{\rm fit} = \langle \sigma v \rangle_{\rm table} / \langle \sigma v \rangle_{\rm fitformula}$.

V. CALCULATIONS AND RESULTS

A. Chemical enrichment and dredge-up as functions of nuclear physics input

Starting from our initial model at the end of core He-burning, we calculate seven full evolutionary sequences that end when all envelope mass is lost and the remaining stellar core is about to become the central star of the planetary nebulae stage. The sequences differ only in the adopted rates for the three reactions investigated here (Table II). One benchmark sequence (ET2) has been computed with the recommended NACRE rates for all three reactions. In addition, six sequences have been calculated in which for each of these reactions the rate from the fitting formula is multiplied by the factors given in Table I, which include the small differences between tabulated and fitting formula values. Thus, for each reaction two sequences are computed, one adopting the upper and one adopting the lower bound of the uncertainty range.

In a second set of sequences we have investigated the influence of the revised (smaller) ^{14}N$(p,\gamma)^{15}$O rate. We have considered also simultaneous changes of both this rate and the triple-α rate (Table III). An overview of the reaction-rate choices for the most interesting cases in which the ^{14}N$(p,\gamma)^{15}$O and the triple-α rates have been changed is shown in Fig. 4.

We summarize these results in Tables II and III. The most salient features of these results are described by the efficiency of dredge-up, λ, and the yield of carbon $p^{\rm e}_{^{12}{\rm C}}$. The efficiency is given by $\lambda = \Delta M_{\rm dup}/\Delta M_{\rm H}$, where $\Delta M_{\rm H}$ is the core mass growth between two He-shell flashes that is due to H-shell

TABLE II. Results for NACRE recommended rates and uncertainties.

ID	Reaction	Factor	$N^{\rm a}_{\rm TP}$	$\lambda(m_c = 0.56\ {\rm M}_\odot)^{\rm b}$	$\lambda^{\rm c}_{\rm max}$	$\sum M_{\rm dup}/10^{-2}\ {\rm M}^{\rm d}_\odot$	$p^{\rm e}_{^{12}{\rm C}}$
ET2	All	1.00	8	0.16	0.29	1.2	2.19
ET5	^{14}N(p,γ)	1.33	9	0.15	0.31	1.2	1.95
ET8	^{14}N(p,γ)	0.75	11	0.29	0.39	2.3	4.27
ET6	3α	1.13	10	0.31	0.41	2.5	5.42
ET9	3α	0.82	7	0.12	0.29	1.1	1.79
ET7	^{12}C(α,γ)	1.44	9	0.24	0.34	1.6	2.71
ET10	^{12}C(α,γ)	0.60	8	0.21	0.33	1.5	3.12

[a]Number of thermal pulses that cause dredge-up.
[b]Dredge-up efficiency λ at mass coordinate 0.56 M$_\odot$; for details see text.
[c]Maximum λ reached by any flash in the entire sequence.
[d]Entire mass dredged up by all dredge-up events.
[e]^{12}C yield from thermal pulses and the accompanying dredge-up in units of 10^{-3} M$_\odot$. For details see text.

TABLE III. Results for revised $^{14}N(p,\gamma)^{15}O$ range.

ID	$^{14}N(p,\gamma)$	3α	N_{TP}^{a}	$\lambda(m_c = 0.56\,M_\odot)$	λ_{max}	$\sum M_{dup}/10^{-2}\,M_\odot$	$p^{e}_{^{12}C}$
ET12	0.75	1.13	10	0.33	0.43	2.5	5.65
ET13	0.64	1.00	9	0.29	0.41	2.2	4.62
ET14	0.64	1.13	11	0.36	0.44	2.9	6.02
ET15	0.54	1.13	11	0.41	0.46	3.2	6.98
ET17	0.54	0.82	9	0.25	0.39	2.3	5.29
ET18	0.75	0.82	8	0.16	0.41	1.8	3.98

[a]See Table II and text for explanations and details.

burning and ΔM_{dup} is the dredged-up mass following the He-shell flash. For each flash, λ indicates the efficiency of dredge-up: $\lambda = 1$ means that the same amount of mass by which the core grew between two flashes is dredged up after a flash. The ^{12}C yield from thermal pulses and the accompanying dredge-up is given for $i = {}^{12}C$ by: $p_i = \int_{M_f}^{M_i} [X_i(m) - X_{ini}]\,dm$, where M_i and M_f are the initial and the final stellar masses at the beginning and the end of the AGB phase, X is the mass fraction at the surface as the star evolves, and X_{ini} is the initial mass fraction. We also tabulate the total dredged-up mass.

The chemical evolution of AGB giants depends sensitively on the rates of the $^{14}N(p,\gamma)^{15}O$ and the triple-α reaction. Calculations with a smaller $^{14}N(p,\gamma)^{15}O$ rate (case ET8) show a larger dredge-up efficiency, a larger dredged-up mass, and a larger amount of carbon mixed from the processed layers to the envelope and a larger carbon yield.[4] All these quantities are about a factor of 2 higher than for the benchmark case.

For the triple-α reaction we observe the opposite behavior. The case ET6 with a larger rate has, on average, He-shell-flash peak luminosities (not shown in the table) that are 20%–50% higher than the benchmark case, and accordingly dredge-up is deeper. The efficiency, total dredged-up mass, and the ^{12}C yield are about a factor of 2 higher for sequence ET6 compared with those of sequence ET2. It is also clear that these effects are nonlinear in the rates. The changes for increases in the $^{14}N(p,\gamma)^{15}O$ rate and decreases in the triple-α rate are small.

The uncertainty in the $^{12}C(\alpha,\gamma)^{16}O$ as given in the NACRE compilation rate has a much smaller influence on the observables studied here. We find that in both cases with upper and lower range values for this rate (cases ET7 and ET10) the ^{12}C yield is somewhat larger than in the benchmark case. Sequence ET10 has a slightly larger ^{12}C yield than ET7, although ET7 has a slightly larger dredge-up mass and efficiency than ET10 (see discussion in Subsec. V B).

In Table III we show the results for the revised $^{14}N(p,\gamma)^{15}O$ rate and for cases in which two rates are changed simultaneously. The ^{12}C yield increases further for the lower $^{14}N(p,\gamma)^{15}O$ rate, and the combination with an increased triple-α rate leads to still larger values. A compact representation of the set of simulations is given in Fig. 5. The main result is that, because of the revision of the $^{14}N(p,\gamma)$ rate, the predicted ^{12}C yields of low-mass stars are about twice as large as with the old rate. In addition, the relative error of the combined effect of the $^{14}N(p,\gamma)$ and triple-α rate has decreased.

The evolution of the ^{12}C abundance is useful to further illustrate the differences. In Fig. 6 the envelope ^{12}C abundance increases in discrete steps for all cases. These steps correspond to the discrete dredge-up events after sufficiently strong He-shell flashes. The astrophysical yield is obtained by integration of the surface abundance over the mass lost. Most notable is the fact that ^{12}C abundances for the shown cases span a range significantly exceeding a factor of 2. Until the reaction rates are better known this is an unavoidable uncertainty in the yield predictions.

These results confirm our original qualitative expectations. A smaller $^{14}N(p,\gamma)^{15}O$ rate leads with a smaller helium production rate and later ignition of the He-shell flash. This flash is then more violent and the subsequent dredge-up is more efficient compared with a case with a larger $^{14}N(p,\gamma)^{15}O$ rate. More efficient dredge-up leads to a larger envelope enrichment, and thus the envelope ^{12}C abundance and stellar yield is larger for the run with the smaller $^{14}N(p,\gamma)^{15}O$ rate. For the triple-α reaction a larger rate leads to stronger He-shell flashes. In fact, the run with the large rate shows He-burning peak luminosities that are about 20%–50% larger than for the run with the lower triple-α rate. Accordingly the run with the larger rate shows greater efficiency, deeper dredge-up, and larger ^{12}C abundances at the surface and in the yields.

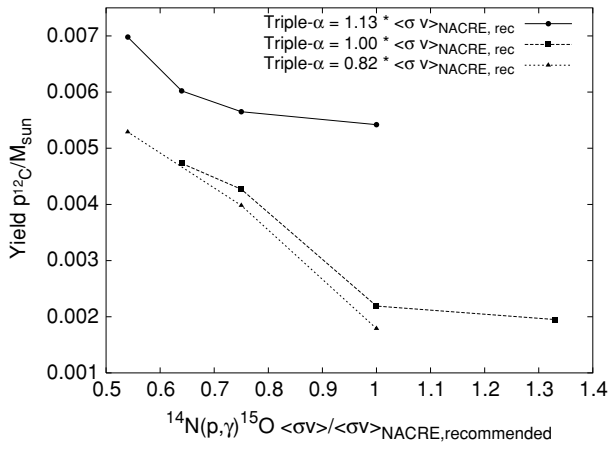

FIG. 5. Overview of ^{12}C yields as functions of the $^{14}N(p,\gamma)$ and triple-α rate, for our $M = 2\,M_\odot$, $Z = 0.01$ TP-AGB models as functions of nuclear reaction rates. Each point refers to the yield of one full stellar evolution model sequence. Lines connect points with the same triple-α rate.

[4]The carbon enrichment is used here as a proxy for the envelope enrichment with nuclear processed material that would include the *s*-process elements, for example.

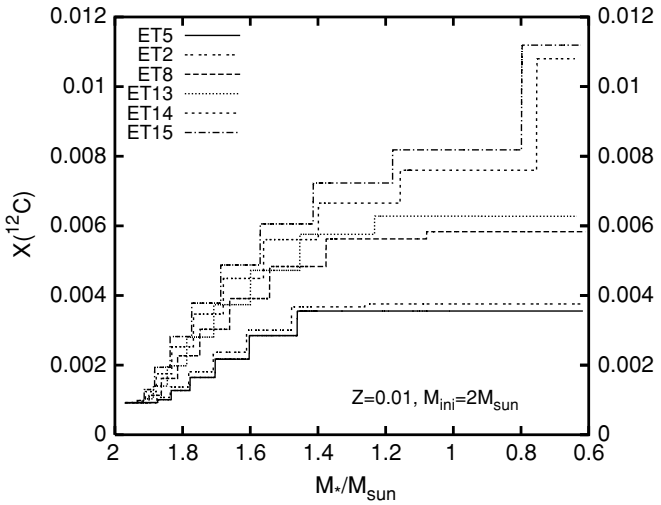

FIG. 6. As in Fig. 3 for sequences with different nuclear reaction rates (Fig. 4). The yields of these sequences are given in Tables II and III.

B. Verification of stellar modeling results

The main set of models was computed with the EVOL stellar evolution code [16]. To check these results we repeated a subset of the numerical experiments with the independent MSSSP code [11]. Calculations were carried out for $M = 2.1$ $M_\odot$ and $Z = 0.008$ with the standard $^{14}N(p,\gamma)$ rate used in that code (very similar to the NACRE rate) starting from the main sequence and a comparison calculation starting, as with the EVOL set of sequences, after the end of core He-burning with 0.6 times the standard $^{14}N(p,\gamma)$ rate. This calculation shows deeper dredge-up and a larger C yield compared with the sequence with the higher $^{14}N(p,\gamma)$ rate. The effect seen in the MSSSP calculations is qualitatively and quantitatively consistent with the EVOL results.

In several test calculations we discovered that starting the comparison runs with different reaction rates at or even after the onset of the He-shell flashes did not show consistent trends. The luminosities of the H- and He-shells depend on the core properties (im particular mass and radius) that are the result of the previous core-burning phases of H and He. For the main set of comparative calculations we therefore choose an initial model about 20 million yr before the first thermal pulse and immediately after the end of the He-core burning.

Comparison calculations have been done with the MSSSP code with different $^{12}C(\alpha,\gamma)^{16}O$ rates. As with the EVOL calculations reported in Subsec. V A, we were not able to identify clear correlations between this reaction rate and the dredge-up and yield properties of the models. The differences we found were below the 10%–15% level and more sensitive to numerical parameters (such as the spatial and temporal resolution) than the $^{12}C(\alpha,\gamma)^{16}O$ rate. (This is actually to be expected, because this reaction rate is not as important as the triple-α rate during the AGB thermal pulse evolution.) The quantities like total dredge-up mass and carbon yield are the results of a discrete process repeated $n \approx 8$–11 times. Thus these numbers are subject to a statistical fluctuation of $\sim 1/n$.

C. The pre-AGB evolution: H- and He-core burning

The main emphasis of this study is the impact of nuclear reaction rates on the AGB evolution, in particular the chemical enrichment through the third dredge-up. However, we did check how the dredge-ups of models with different reaction rates change if run all the way from the main sequence, including the effect on H- and He-core burning. One test was done with the MSSSP code, starting a sequence with the reduced $^{14}N(p,\gamma)$ rate from the main sequence. In that sequence the dredge-up during the AGB thermal pulse phase is still significantly larger than with the NACRE recommended rate, but the increase is somewhat smaller then for the comparison runs started after the end of He-core burning.

A second test was made with the EVOL code running two sequences all the way from the zero-age main sequence to the end of the thermal pulse AGB. In addition to the benchmark case ET2, we reran the rate combination of case ET14 [$0.64 \times$ $^{14}N(p,\gamma)$, $1.13 \times 3\alpha$], and we refer to this run as ET14a. We found that in this case the dredge-up is about 20% larger than in the ET14 model calculated from the starting model after the end of He-core burning. This is another example of the highly nonlinear behavior of the third dredge-up.

We can analyze the differences caused by the change of nuclear reaction rate on the H- and He-core-burning phases and find them to be very small. The central temperature during the H-core burning of the 2 $M_\odot$ models studies here are 2.1×10^7 K initially, increasing sharply to 3.45×10^7 K at the end of H-core burning. Case ET14a shows central temperatures throughout core H-burning that are 1% larger than those of the benchmark case. This small increase of temperature is sufficient to increase energy generation required for hydrostatic equilibrium because of the steep temperature dependence of the $^{14}N(p,\gamma)$ rate. Run ET14a consumes H in the center slightly faster, and accordingly the H-core-burning phase is about 1% shorter than in the benchmark case. The mass of the convective core is practically the same in both cases. None of these nuclear reaction-rate differences during the main-seqeunce evolution would make an observable difference.

During the He-core burning, the slightly larger triple-α rate leads to a slightly larger C/O ratio on the core (2%). However, during the EVOL calculations some breathing pulses of the convective core occur. These breathing pulses are well known during the He-core-burning phase and are related to the unstable growth of the convective core into a layer that is stabilized by a composition gradient. The treatment of convective boundaries implemented in the EVOL code makes the occurrence of breathing pulses somewhat dependent on the numerics. It is not clear from the calculations to what extent the magnitude of the central C/O ratio depends on this simulation error. However, since the effect is small we decided not to follow this question any further. At the end of He-core burning the age difference between the two runs is 0.3% of the total age. The core mass and size are practically identical.

The second dredge-up decreases the core mass slightly for stars of this mass. This effect is weaker in run ET14a, so that the core mass after the second dredge-up is slightly larger than in the benchmark run. It is during the early AGB evolution from the end of He-core burning to the first thermal pulse that sequence ET14a has a slower growth rate of the H-free

core, corresponding to a 3% smaller H-burning luminosity. This leads to a 2% smaller core mass at the first thermal pulse for case ET14a compared with that of the benchmark run. A smaller core mass should result in a less efficient third dredge-up, if the reaction rates are the same. However, ET14a has a combination of rates that increases the third dredge-up, as shown in the main set of comparative calculations. In addition, because the stellar luminosity of run ET14a is somewhat smaller, the mass loss according to the adopted L-dependent mass loss formula is smaller, and the thermal pulse AGB phase is longer by 15%. In particular, the last thermal pulses have a larger He-flash peak luminosity that, as discussed above, leads to more efficient dredge-up.

The third test concerns the influence of the $^{12}C(\alpha,\gamma)^{16}O$ rate on the pre-AGB evolution. We calculated an additional sequence (ET7a) corresponding to sequence ET7 (NACRE rate times 1.44) from the main sequence to the thermal pulse AGB phase. As can be expected, there are no differences (e.g., duration, core size) between run ET7a and run ET2a during the H-core-burning phase. During the He-core-burning phase the central C/O ratio is systematically smaller in run ET7a compared with that of the benchmark case. For example, after 1/3 of the He-core-burning phase, $C/O = 3.6$ for the ET7a run and $C/O = 5.2$ for the benchmark case. Not surprisingly, the ratio of those two values is 1.44. The ET2a He-core-burning duration is 3% shorter than that of ET7a; the central temperature and density are almost the same. As in the discussion of run ET14a above, we note the occurrence of breathing pulses during the He-core-burning phase, in particular toward the end of this phase. In runs ET2a and ET7a these breathing pulses are very similar, with no observable difference. The core mass at the first thermal pulse is 0.494 $M_\odot$ for ET7a, and practically the same (0.493 $M_\odot$) for ET2a. We continued run ET7a into the thermal pulse regime until the onset of the third dredge-up. As expected from the practically idenitical core masses, the ET7a and ET2a sequences show very similar third dredge-up behavior.

In conclusion, we find that, as expected, the sensitivity of stellar evolution properties to the $^{12}C(\alpha,\gamma)^{16}O$ rate during the H- and He-core-burning phases of low-mass stars is small. There is a small dependence of the thermal pulse AGB results on the progenitor evolution, which, however, does not change the trends established with our main set of comparative calculations starting with the same initial model after the end of He-core burning.

VI. IMPROVING THE TRIPLE-α RATE

The recent results of Refs. [33,34] have shown that, for $T = 0.1 - 100 \times 10^8$ K, the triple-α reaction rate is dependent essentially on the properties of the O^+ state at an excitation energy of 7.65 MeV in ^{12}C, the Hoyle state. This reduces the problem of determining the triple-α rate to determining the properties of that state.

Because the 7.65-MeV state is a O^+ state, its direct excitation is difficult. Moreover, the ratio of the radiative width to the total width is small, 4.13×10^{-4}. As a result one must determine Γ_{rad} from the relationship

$$\Gamma_{rad} = \Gamma_\gamma + \Gamma_\pi = \frac{\Gamma_\gamma + \Gamma_\pi}{\Gamma}\frac{\Gamma}{\Gamma_\pi}\Gamma_\pi. \qquad (2)$$

Here Γ_γ, Γ_π, and Γ are the γ width, pair width, and total width, respectively, of the 7.65-MeV state. Each of the three factors on the right-hand side is determined in a separate experiment. At present they are known with an accuracy, left to right, of $\pm 2.7\%$, $\pm 9.2\%$, and $\pm 6.4\%$. In all cases, there are several consistent measurements, so these results can be regarded as robust.

There are two new developments that may significantly improve our knowledge of Γ_{rad}, and hence the triple-α reaction rate, by improving the accuracy of the poorest known quantities: the pair width Γ_π and the pair branch Γ_π/Γ. The pair width is determined from the transition charge density for inelastic electron scattering to the 7.6-MeV state. There is a new, as yet unpublished result [43], based on a compendium of extant measurements over a large momentum transfer range, that has a quoted accuracy of $\pm 2.7\%$. It is difficult to imagine that a more accurate value of Γ_π can be obtained. On the other hand, this value is not quite consistent with the earlier values of Γ_π.

The pair branch Γ_π/Γ is the least well-known quantity, primarily because it is so small, about 6×10^{-6}. A new experiment [44], a Western Michigan University and Michigan State University collaboration, is underway that uses the tandem accelerator at Western Michigan University. The proposed detector is an improved version of that used in Ref. [45].

In this experiment the 7.6-MeV state in ^{12}C is excited by inelastic proton scattering, taking advantage of a strong resonance at an excitation energy of 10.6 MeV and a scattering angle of 135° in the lab. To reduce γ-ray backgrounds, a coincidence is required between a thin plastic-scintillator cylinder surrounding the target and a large plastic scintillator surrounding both the target and the cylinder. This arrangement should strongly discriminate against γ-ray backgrounds—γ rays have only a small probability of interacting in the thin cylinder. The pair branch is then given simply by the ratio of the number of positron-electron pairs detected by plastic-scintillator coincidences to the number of counts in the 7.65-MeV peak in the proton spectrum. An examination of the systematic uncertainties in the similar Robertson experiment leads us to estimate that an accuracy of 5% is achievable.

These two results promise to reduce the uncertainty in the triple-α rate to about 6%; as we have seen, that will greatly improve the reliability of predictions of carbon production in AGB stars.

VII. DISCUSSION

We have presented a systematic investigation of the propagation of the rate uncertainties of key nuclear reaction rates into chemical enrichment predictions of low- and intermediate-mass stars that have reached the thermal pulse AGB phase. We found that the dredge-up in low-mass stars depends rather sensitively on the adopted reaction rates. The overall dredge-up of material and, specifically, the yield of ^{12}C have uncertainties of greater than a factor of 2 owing to the reaction-rate uncertainties. The C/O ratio at the stellar surface has a similar uncertainty.

Such uncertainties are a problem for many problems of current astrophysical interest. The construction of integrated models of galactic chemical evolution, for example, includes contributions from stars of all initial masses [46], and AGB

stars are important contributors for some nuclear species. The enrichment of the surface abundance with carbon also effects the appearance of AGB stars in extragalactic stellar population studies. As the surface abundance changes from O dominated (C/O < 1) to C rich (C/O > 1), the molecular chemistry in the giant's atmosphere changes considerably [47], affecting the star's surface temperature and thereby its astronomical colors. In older extragalactic populations, AGB stars are often the brightest stars and can probe the population's properties, for example, its age. Finally, many extremely metal-poor (EMP) stars, which may provide information on chemical evolution in the early universe, turn out to have binary white dwarf companions [48]. The unusual abundance patterns of these EMP stars [49] should correlate with the chemical yields of the white dwarf progenitors—the AGB stars at this low metallicity.

Of course nuclear reaction rates are not the only uncertainties in AGB models. The treatment of convection, and mixing in general, affects the efficiency of the third dredge-up as well [8,50]. Two separate issues have to be considered. Convection in one-dimensional stellar evolution models is usually approximated by some variant of the local mixing-length theory [51]. In this ballistic theory the mean free path of rising and descending blobs has to be specified.[5] From the sparse information on this topic in the literature [18,52,53] we roughly estimate that the mixing-length uncertainty translates into yield uncertainties ranging from 30% to a factor of a few, depending on initial stellar mass.

Another source of uncertainty of dredge-up predictions is the treatment of convective overshooting. There is now enough numerical and experimental proof to claim that convective overshooting takes place in stellar environments and that the efficiency of that process depends on the evolutionary phase [54]. It appears that dredge-up predictions are uncertain by a factor of 2 because of the poorly known overshooting efficiency.

These two issues related to the modeling of stellar convection have been viewed as the major source of dredge-up and yield prediction uncertainties. Our study shows that nuclear reaction-rate uncertainties of two key reactions induce modeling uncertainties of similar magnitude. The need to reduce these uncertainties is a powerful argument for better determinations of the reaction rates of the $^{14}\mathrm{N}(p,\gamma)^{15}\mathrm{O}$ and triple-α reactions. Progress in experimental nuclear physics will have an immediate impact on astrophysical models that rely on stellar yields.

[5]Usually one uses the well-known stellar parameters of the sun to calibrate this free parameter and keeps this value constant as the evolution progresses. However, multi-dimensional hydrosimulations have shown that this assumption is not correct [52], and for evolved giants the mixing-length parameter may be larger by some substantial fraction.

ACKNOWLEDGMENTS

This work was funded in part under the auspices of the U.S. Department of Energy and supported by its contract W-7405-ENG-36 to Los Alamos National Laboratory, the Australian Research Council, and by U.S. National Science Foundation grants PHY01-10253 and PHY02-16783, the latter funding the Joint Institute for Nuclear Astrophysics, a National Science Foundation Physics Frontier Center.

[1] S. E. Woosley, A. Heger, T. Rauscher, and R. D. Hoffmann, Nucl. Phys. **A718**, 3 (2003).
[2] J. A. Stoesz and F. Herwig, Mon. Not. R. Astron. Soc. **340**, 763 (2003).
[3] G. R. Huss, A. J. Fahey, R. Gallino, and G. J. Wasserburg, Astrophys. J. **430**, L81 (1994).
[4] L. R. Nittler, C. M. O. Alexander, X. Gao, R. M. Walker, and E. Zinner, Astrophys. J. **483**, 475 (1997).
[5] F. Herwig and S. M. Austin, Astrophys. J. Lett. **613**, L73 (2004).
[6] I. Iben, Jr. and A. Renzini, Annu. Rev. Astron. Astrophys. **21**, 271 (1983).
[7] J. Lattanzio and M. Forestini, in *AGB Stars*, edited by T. L. Bertre, A. Lebre, and C. Waelkens (Astronomical Society of the Pacific, 1999), IAU Symp. 191, p. 31.
[8] F. Herwig, Annu. Rev. Astron. Astrophys. **43**, 435 (2005).
[9] D. Schönberner, Astron. Astrophys. **79**, 108 (1979).
[10] I. Iben, Jr., Astrophys. J. **246**, 278 (1981).
[11] J. C. Lattanzio, Astrophys. J. **311**, 708 (1986).
[12] D. Hollowell and I. Iben, Jr., Astrophys. J. **333**, L25 (1988).
[13] E. Vassiliadis and P. Wood, Astrophys. J. **413**, 641 (1993).
[14] T. Blöcker, Astron. Astrophys. **297**, 727 (1995).
[15] N. Mowlavi, Astron. Astrophys. **344**, 617 (1999).
[16] F. Herwig, Astron. Astrophys. **360**, 952 (2000).
[17] A. I. Karakas, J. C. Lattanzio, and O. R. Pols, Pub. Astrom. Soc. Aust. **19**, 515 (2002).
[18] A. I. Boothroyd and I.-J. Sackmann, Astrophys. J. **328**, 671 (1988).
[19] K. H. Despain and J. M. Scalo, Astrophys. J. **208**, 789 (1976).
[20] C. Angulo *et al.*, Nucl. Phys. **A656**, 3 (1999), NACRE compilation.
[21] U. Schroeder, H. W. Becker, G. Bogaert, J. Görres, C. Rolfs, H. P. Trautvetter, R. E. Azuma, C. Campbell, J. D. King, and J. Vise, Nucl. Phys. **A467**, 240 (1987).
[22] E. G. Adelburger *et al.*, Rev. Mod. Phys. **70**, 1265 (1998).
[23] B. A. Brown (private communication).
[24] P. F. Bertone, A. E. Champagne, D. C. Powell, C. Iliadis, S. E. Hale, and V. Y. Hansper, Phys. Rev. Lett. **87**, 152501 (2001).
[25] K. Yamada *et al.*, Phys. Lett. **B579**, 265 (2004).
[26] C. Angulo and P. Descouvement, Nucl. Phys. **A690**, 755 (2001).
[27] A. M. Mukhamedzhanov *et al.*, Phys. Rev. C **67**, 065804 (2003), and private communication.
[28] A. Formicola *et al.*, Phys. Lett. **B591**, 61 (2004).
[29] R. C. Runkle, A. E. Champagne, C. Angulo, C. Fox, C. Iliadis, R. Longland, and J. Pollanen, Phys. Rev. Lett. **94**, 082503 (2005).
[30] S. O. Nelson, M. W. Ahmed, B. A. Perdue, K. Sabourov, A. L. Sabourov, A. P. Tonchev, R. M. Prior, M. Spraker, and H. R. Weller, Phys. Rev. C **68**, 065804 (2003).
[31] H. Costantini *et al.*, Nucl. Phys. **A758**, 383c (2005).

[32] J. A. Nolen, Jr. and S. M. Austin, Phys. Rev. C **13**, 1773 (1976).
[33] H. O. U. Fynbo *et al*., Phys. Rev. Lett. **91**, 082502 (2003).
[34] H. O. U. Fynbo *et al*., Nature (London) **433**, 136 (2005).
[35] M. F. E. Eid, B. S. Meyer, and L.-S. The, Astrophys. J. **611**, 452 (2004).
[36] L. Buchmann, Nucl. Phys. **A758**, 355c (2005).
[37] J. W. Hammer *et al*., Nucl. Phys. **A758**, 363c (2005).
[38] R. Kippenhahn and A. Weigert, *Stellar Structure and Evolution* (Springer, Berlin, 1990).
[39] F. Herwig, Astrophys. J. **605**, 425 (2004).
[40] C. A. Iglesias and F. J. Rogers, Astrophys. J. **464**, 943 (1996).
[41] D. Alexander and J. Ferguson, Astrophys. J. **437**, 879 (1994).
[42] F. Herwig, T. Blöcker, D. Schönberner, and M. F. El Eid, Astron. Astrophys. **324**, L81 (1997).
[43] H. Crannell *et al*., Nucl. Phys. **A758**, 399c (2005).
[44] C. Tur, A. Wuosmaa, K.-I. Yoneda, and S. M. Austin (unpublished).
[45] R. G. H. Robertson, R. A. Warner, and S. M. Austin, Phys. Rev. C **15**, 1072 (1977).
[46] F. X. Timmes, S. E. Woosley, and T. A. Weaver, Astrophys. J. Suppl. **98**, 617 (1995).
[47] P. Marigo, Astron. Astrophys. **387**, 507 (2002).
[48] S. Lucatello, S. Tsangarides, T. C. Beers, E. Carretta, R. G. Gratton, and S. G. Ryan, Astrophys. J. **625**, 825 (2005).
[49] T. C. Beers and N. Christlieb, Annu. Rev. Astron. Astrophys. **43**, 531 (2005).
[50] C. A. Frost and J. C. Lattanzio, Astrophys. J. **473**, 383 (1996).
[51] E. Böhm-Vitense, Z. Astrophys. **46**, 108 (1958).
[52] H. Ludwig, B. Freytag, and M. Steffen, Astron. Astrophys. **346**, 111 (1999).
[53] P. Marigo, Astron. Astrophys. **370**, 194 (2001).
[54] F. J. Robinson, P. Demarque, L. H. Li, S. Sofia, Y.-C. Kim, K. L. Chan, and D. B. Guenther, Mon. Not. R. Astron. Soc. **347**, 1208 (2004).